The Use of Bone Char as an Adsorbent for the Treatment of Wastewater Containing Lead and Fluoride

Lerato Keele[1], Peter Osifo[2]

***Abstract*—** Consumption of water from sources contaminated with inorganics such as Pb^{2+} and F^-, cause adverse health effects to people living in undeveloped areas. Adsorption of the inorganics onto bone char renders the water potable. Bone char was synthesized by pyrolysis and characterization techniques used include TGA, FTIR, XRD and XRF. BET showed bone char average pore sizes of 1.383 nm using CO_2 and 10.645 nm using N_2. EDS revealed Ca, P and O as elemental components of bone char. Adsorption isotherms of Pb^{2+} fit the Langmuir model with a maximum adsorption capacity (q_m) of 36.765 mg/g, and adsorption kinetics of F^- fit the first-order model with a kinetic constant (k_1) of 0.014 min^{-1}. The breakthrough curves show rapid adsorption of Pb^{2+} and slow adsorption of F^-. In this work use of bone char as adsorbent was found to be suitable for the removal of Pb^{2+} and F^- from contaminated wastewater.

***Keywords*—**Adsorption, Bone Char, Fixed-Bed Filter, Water Treatment.

I. Introduction

It is known that water is one of the most important commodities to humans. People need it to live because it is involved in numerous bodily systems and functions, therefore, it is important to consume water that is free from contaminants. Consumption of contaminated water has adverse effects on human health. The adverse effects that these contaminants have on humans are numerous and varied and ultimately can cause a deterioration in health. Contaminated water is often consumed by people living in rural and peri-urban communities [1]. This is because there are no developed drinking water and wastewater treatment infrastructures to and from their homes. Therefore, people living in these areas resort to collecting water from various unregulated underground and surface sources. There are three types of contaminants found in water, namely microbial, organic and inorganic, but for this research the type that is of interest is the inorganic contaminants. The dominant groups of inorganic contaminants are heavy metals and some halogens [2]. Heavy metals include Pb, Fe, Hg, Cu, Zn, Cd, Ni and halogens include F, Br and Cl, with Pb and F being the focus for this research. Pb is a ubiquitous heavy metal contaminant in water due to anthropogenic activities. The primary sources of Pb contamination are unauthorized and illegal dumping of effluent from industrial processes such as those of mining, metals smelting and the dumping of Pb containing domestic products such as paint, lead-acid batteries and pesticides in streams and rivers upstream from the rural communities that consume the water from these rivers downstream [3]. Fluoride contamination is widely distributed in the geological environment and generally released into the environment by naturogenic means through slow leaching and dissolution of fluorine containing rocks. Various rocks such as granite, syenite and shale contain fluoride that can be released into the groundwater. Anthropogenic sources contributing to fluoride contamination of surface water due to improper discharge of waste products include industrial processes such as ceramic and glass production, electroplating, brick and iron works, and aluminium smelters [4,5].

Among many removal techniques, adsorption is a very promising method for the removal of heavy metals from water owing to the heavy metal removal efficiency, high adsorption rate, selective removal, and the availability of a wide range of adsorbent materials [6]. Bone char, a blackish material obtained from the thermal treatment (pyrolysis) of bones [7,8], has gained considerable attention as an adsorbent owing to its low cost, ease of preparation, biocompatibility [5] effective filtering and adsorbent material after its activation [8].

II. Methodology

A. Preparation of Bone Char

Bovine bones were purchased from a local butchery in Vanderbijlpark, South Africa. Meat and fat pieces were removed from the bones with a knife. The bones were washed three times by soaking in hot tap water and again twice with ultrapure water, drained and then dried in a drying oven at 105°C overnight. After the bones had dried, they were crushed with a hammer into pieces of ≤ 3 cm in size. The crushed bones were pyrolyzed at 700°C for 1 hour in a rotary kiln furnace to synthesize the bone char. The bone char was then crushed in a ball mill and sieved to particle sizes ranging between 300 and 500 μm.

B. Determination of Acid-Basic Properties of Bone Char

The acid-basic properties of bone char were determined using the point zero charge (PZC) method outlined by [9]. A

Lerato Keele[1] is with the Department of Chemical and Metallurgical Engineering, Vaal University of Technology, Andries Potgieter Blvd, Vanderbijlpark, 1911, South Africa

Peter Osifo[2] is with the Department of Chemical and Metallurgical Engineering, Vaal University of Technology, Andries Potgieter Blvd, Vanderbijlpark, 1911, South Africa

100 ml 0.01 mg/L NaCl solution was prepared and then degassed with N_2 gas to remove and prevent further dissolution of CO_2 . 10 beakers were each filled with 10 ml of the 0.01 mg/L NaCl solution and their pH were adjusted from 1 to 10 with either HCl or NaOH. 10 mg of bone char was added to each beaker and after 24 hrs the final pH of the solutions was measured.

C. Characterization of Bone Char

Different analytical techniques were used to characterize the bone char. The thermal decomposition rate of the bovine bones was determined using a Perkin Elmer Pyris 1 TGA from 30 to 800°C at a heating rate of 10°C/min, with a 20 mg ±2 mg sample in an inert atmosphere of Helium gas. BET analysis for the determination of total surface area, pore size and pore volume of the bone char was done using the Micromeritics 3Flex Adsorption Analyzer. The elemental components of the bone char were determined using the Oxford Xmapzo eds, integrated detector, Spectra at 15kV with Inca software. FTIR was used to identify the functional groups of bone char using the KBr method. The FTIR spectra was measured on the Agilent Cary 630 FTIR, with a wavenumber ranging from 200 cm^{-1} to 4000 cm^{-1} using the MicroLab software. SEM imaging was used to determine the morphology of the bone char using the FEI Quanta FEG 250, Environmental Scanning Electron Microscope. XRD was used to determine the crystallinity, orientation, phase, and percentage crystallinity of bone char. The sample material was prepared for XRD analysis using the backloading preparation method. Diffractograms were obtained using a Malvern Panalytical Aeris diffractometer with PIXcel detector and fixed slits with Fe filtered Co-Kα radiation. The phases were identified using X'Pert Highscore plus software. The relative phase amounts (weights%) were estimated using the Rietveld method. Amorphous phases, if present, were not taken into consideration during quantification.

D. Preparation of Fluoride and Lead Solutions

Analytical grade $Pb(NO_3)_2$ and NaF from Sigma-Aldrich were used to prepare the stock solutions each of 100 mg/L. Working solutions were prepared by dilutions from the stock solution. The concentrations of the Pb^{2+} and F^- ions were determined with an atomic absorption spectroscopy (AAS) and an ion chromatographer (IC), respectively, before and after the adsorption experiments.

E. Batch adsorption and Fixed-Bed Filtration Experiments

Sorption kinetic and isotherm models of bone char for Pb^{2+} and F^- removal were studied in batch adsorption processes where the bone char was contacted with the synthetic contaminant solutions, described in section D, in a glass container at room temperature (25 ±2°C). Kinetics sorption experiments were performed with 250ml solutions and 0.25g of bone char as the adsorbent. 5ml samples were taken at specific time intervals until the equilibrium was reached. Isotherm sorption experiments were performed with 100ml solutions of initial concentrations ranging from 10 to 70mg/L and 0.1g of bone char added to each solution. Final concentrations were determined after the adsorption isotherm experiment ended. All the experiments were run in a shaker incubator at 120 rpm. The samples were filtered before the analysis was done.

Fixed-bed sorption was carried out through a glass column of 38 mm diameter where bone char was packed as 110 mm length fixed-bed and the synthetic contaminated solution was passed through the bone char fixed-bed by gravitational force. A 5 L solution of 10 mg/L $Pb(NO_3)_2$ and 10 mg/L NaF was prepared as the synthetic contaminated solution from the stock solutions described in section D. Samples were taken at time intervals and analyzed with the AAS and IC to determine the effluent concentrations of Pb^{2+} and F^- respectively. The percentages of Pb^{2+} and F^- ions adsorbed onto bone char during treatment through the fixed-filtration-bed were calculated using (1), expressed in the following way:

$$\text{Removal } (\%) = \frac{C_0 - C_f}{C_0} \times 100 \quad (1)$$

where C_0 and C_f are the initial and final concentrations (mg/L) of the contaminants in solution, respectively.

III. RESULTS AND DISCUSSION

A. Characterization of Bone Char Before and After Adsorption

The thermogravimetric analysis of bone char as shown in Figure 1, gives two stages of weight loss from the TGA curve (wt%). The first stage is from 32 to 200 ^{0} C, indicated by the first DTG peak with a maximum mass loss rate of 2.3 %/min. This is the dehydration stage where a 9% weight loss due to evaporation of water bound to the bone structure takes place, as corroborated by [10,11]. The second stage is from 200 to 650 ^{0} C, indicated by the second DTG peak with a maximum mass loss rate of 24 %/min, and is in agreement with what [10–12] report to be the decomposition stage. A portion of the third stage is seen from 650 ^{0} C to a temperature that is above 900 ^{0} C but that was not fully observed due to the TGA run cycle ending at 900 ^{0} C. Conclusively only 2 complete stages can be observed.

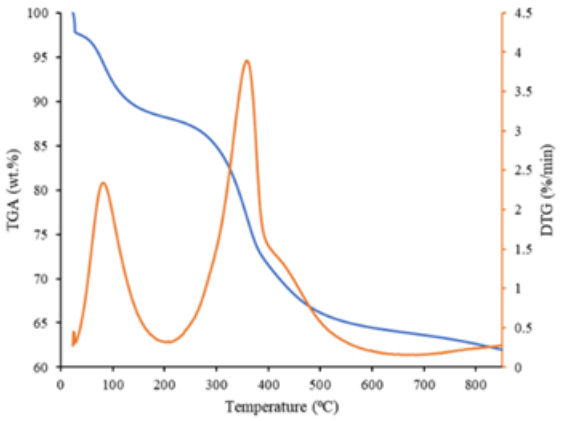

Fig. 1 *Thermogravimetric analysis of bovine bone*

The elemental composition of bone char before adsorption is indicated from the EDS bar graph in Figure 2(a). The basic elemental components that make up the calcium hydroxyapatite structure (Ca, P and O), which is the main component of bone char, are all present at fairly high atomic percentages in the bone char, except the H elemental component which is generally

undetectable by EDS analysis due to its low atomic number. The hydroxyapatite composition can be confirmed by the ratio of the atomic% of Ca/P, as seen from the chemical properties listed in Table 1. The Ca/P ratio was calculated to be 2.39, which is within the reported 2.46 to 2.06 ratio range of bone chars obtained at temperatures between 650 and 1000°C, and the bone char for this research was prepared at 700°C. The EDS graph in Figure 2(b) is of bone char after adsorption of Pb^{2+} ions. The adsorbed Pb^{2+} ions account for 38.59 atomic% of the elemental components of the bone char whereas the Ca elemental component was reduced to 18.09 atomic% which is below half of what was detected in the bone char before Pb^{2+} adsorption. This indicates that Pb^{+2} ions were incorporated into the bone char possibly by ion exchange with Ca^{2+} ions from the $Ca_5(PO_4)_3OH$ molecules of the bone char to form $Pb_5(PO_4)_3OH$. Figure 2(c) is the EDS bar graph of the elemental components of bone char after adsorption of F^- ions. The fluoride elemental component that was adsorbed onto bone char was 1.16 atomic%. This low atomic% could be because of the repulsive forces due to the same negative ionic charges of the bone char and F^- ions.

The physical properties of bone char were determined using BET surface area analysis. Analysis was done separately with two different inert gas environments and the results can be compared in Table I. The inert environment provided by the N_2 gas gave better results across the board in that the total surface area, average pore size and pore volume had higher values than those produced from the CO_2 gas. This basically means that the bone pyrolyzed in a N_2 gas environment would result in bone char that can possibly adsorb more contaminants out of solution than that of bone char pyrolyzed in a CO_2 gas environment. This translates to N_2 gas produced bone char having more binding sites on and within the pores of its surface. By calculating the differences in each of the physical properties obtained from both gases it can be seen that N_2 gas produces bone char with a: total surface area that is 37.2693 m2/g more than that of its counterpart, average pore size that is 9.262 nm more, pore volume that is 0.1961 cm3/g more than that of CO_2. However, the physical properties of N_2 gas pyrolyzed bone char reported by [11] which was pyrolyzed at 700 ^{0} C gave a higher total surface area at 110 m^2/g, higher pore volume at 0.233 cm^3/g, with a lower average pore size of 8.47 nm. The differences in physical properties of the N_2 gas pyrolyzed bone chars in this research and that of [11] is not too vast and it could be due to differences in the heating rate and the residence time used on the respective furnaces.

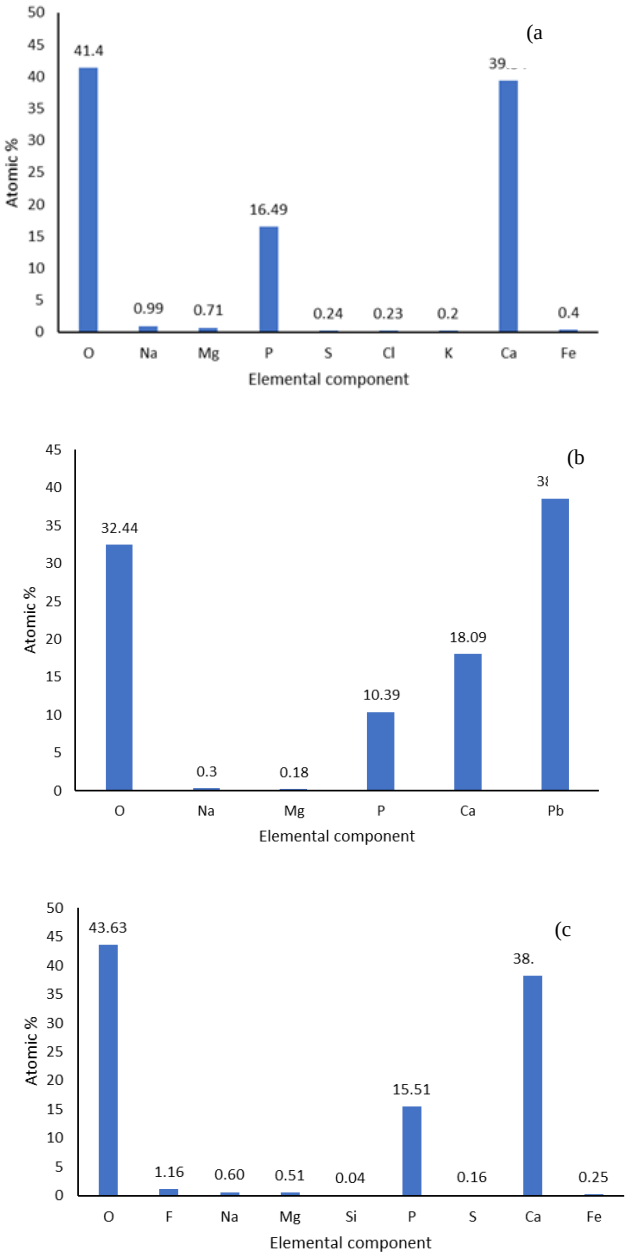

Fig. 2 : EDS results of bone char (a) before adsorption, (b) after lead adsorption and (c) after fluoride adsorption

TABLE I
PHYSISCAL AND CHEMICAL PROPERTIES OF BONE CHAR

	Bone char	
Chemical properties		
Phosphorus	16.49%	
Calcium	39.34%	
Ca/P	2.39	
Physical properties	CO_2	N_2
Total surface area	41.864 m^2/g	79.133 m^2/g
Average pore size	1.383 nm	10.645 nm
Pore volume	0.0145 cm^3/g	0.211 cm^3/g

The FTIR spectra in Figure 3 shows some major bands that are indicative of the presence of functional groups of bone char according to a data base by [13]. The 4 bands that are commonly mentioned by most authors are at 567, 605, 1037, and 3441

cm^{-1}. The bands at 567 and 605 cm^{-1} are indicative of the asymmetric bending mode of vibration between P and O in PO_4^{3-}. The band at 1037 cm^{-1} is of the asymmetric stretching mode vibration of PO_4^{3-}. The band at 3441 cm^{-1} is indicative of the OH stretching vibrations mode. Other bands that should be noted are at 1454 cm^{-1} indicating the asymmetric stretching vibration between C and O of the CO_3^{2-} group, at 1643 cm^{-1} indicating the asymmetric bending vibration mode of OH groups, and at 2924 cm^{-1} indicating the methyl groups of bone char.

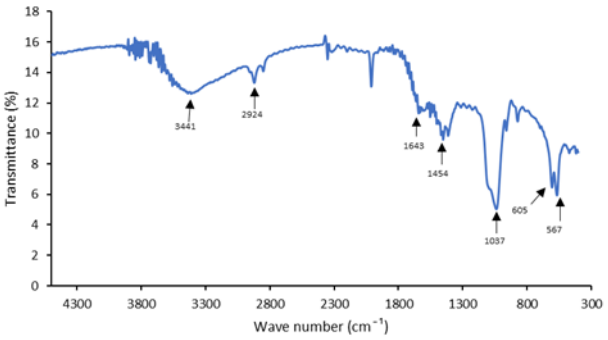

Fig.3 *FTIR spectra of bone char*

The XRD results of the bone char before adsorption can be seen in the diffractogram in Figure 4(a) which demonstrates that the sample was determined to be 100% by weight percentage $Ca_5(PO_4)_3(OH)$ semicrystalline molecular structure. The diffractogram peaks that confirm that the compound is $Ca_5(PO_4)_3(OH)$ can be seen at 2θ 25.371^0, 37.101^0, 46.643^0, 54.824^0 and 58.100^0 which correspond to the Miller indices {020}, {121}, {310}, {222} and {123} respectively. These are the Miller indices that correspond to the XRD diffraction peaks that have been previously reported by other researchers such as [14–16]. The Miller indices planes of $Ca_5(PO_4)_3(OH)$ match a hexagonal shape of the crystalline structure. The XRD diffractogram in Figure 4(b) is of bone char after Pb^{2+} ion absorption and the peak at 2θ 35^0 confirms the presence of Pb^{2+} ions absorbed onto bone char, which is similar to what [17] had reported and when compared to the XRD diffractogram on Figure 4(a) it can be seen that there was an absence of Pb^{2+} ions due to the absence of the peak at 2θ 35^0. The Pb^{2+} ions comprised a weight percentage of 2.1% with the rest of the bone char sample comprising $Ca_5(PO_4)_3OH$ at 97.9% weight percentage and the molecular structure is semicrystalline. The Pb^{2+} ion adsorption onto bone char was most probably due the ion exchange with the Ca^{2+} ions of the $Ca_5(PO_4)_3$ molecule to form $Pb_5(PO_4)_3OH$.

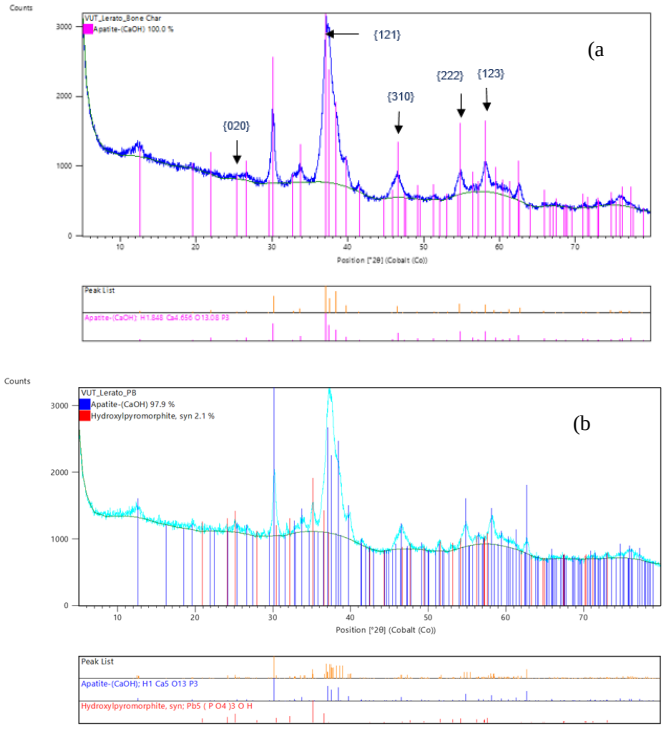

Fig. 4 XRD difffractogram of bone char before (a) and after (b) lead adsorption

B. Acid-Basic Properties of Bone Char

Figure 5 is a graph showing the acid-basic properties of bone char. Where the initial and final pH values intercept is where the PZC pH can be found. The PZC of this bone char was determined to be 6.18 and this means that when solution of contaminants has a pH value below 6.18 the bone char will have a positive charge and a higher affinity for adsorbing anions out of solution. When the solution of contaminants has a pH value above 6.18, the bone char will have a negative charge and a higher affinity for adsorbing cations out of solution. The PZC pH of this bone char is in the range of many that have been reported in literature by [5,15,18,19], with PZC between 4.5 and 8.4.

C. Isotherm Modelling

To determine the best fitting adsorption isotherm and kinetics models for lead and fluoride adsorption, the adsorption experiments were conducted in glass beakers in batch form. The linearized forms of the Langmuir and Freundlich isotherm models can be seen in Figure 6 (a) & (b), respectively, and Table II contains the adsorption isotherm parameters. From Figure 6 (a) Pb^{2+} adsorption fits the linear Langmuir isotherm better with an $R^2 = 0.964$. This means that the adsorption of the Pb^{2+} ions on the bone char is in a monolayer form on adsorption sites that are homogenously distributed on the

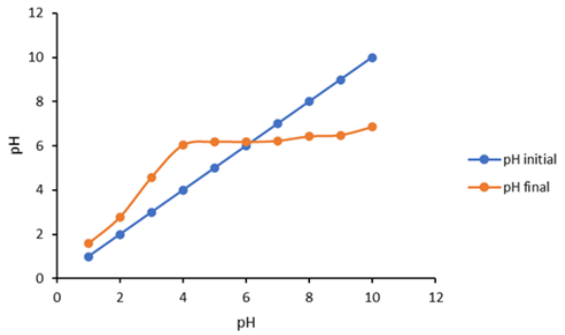

Fig. 5 Acid-basic properties of bone char

surface of the bone char, the Pb^{2+} adsorbates don't have interparticle attraction, and that the adsorption energy is constant throughout all the adsorption sites. The maximum adsorption capacity (q_m), determined from the gradient of the linearized Langmuir model is 36.765 mg/g. The Langmuir constant (b), determined from the slope of the graph, indicates the binding affinity of the adsorbent to the adsorbate and a high b value translates to a high affinity. In this research b = 0.365 has a higher affinity compared to b = 0.173 from [16] but is lower than b = 0.503 from [20]. The adsorption of F^- ions onto bone char, shown in Figure 6 (b) fit the linear Freundlich isotherm better with an $R^2 = 0.999$. This means that adsorption of F^- fits a reversible multi-layered process on a heterogenous surface where the maximum adsorption capacity k_f = 1.008 mg/g and the adsorption affinity ($\frac{1}{n}$) = 1.160 meaning the adsorption is favourable because of the n value being less than 1.

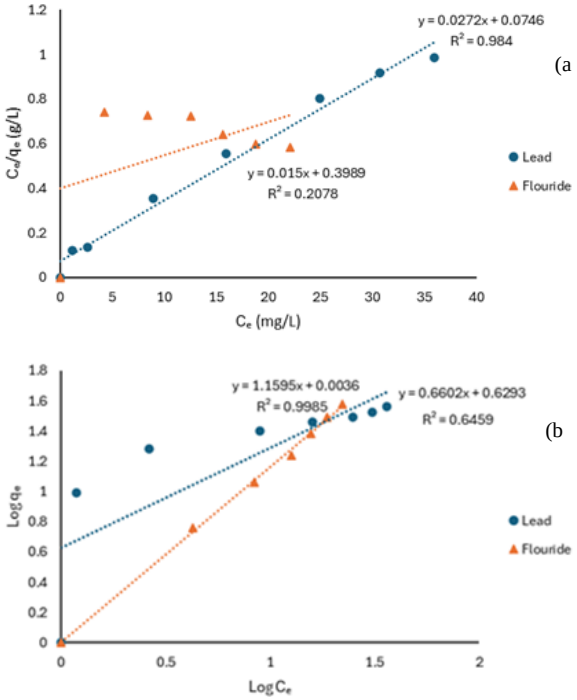

Fig. 6 Linear Langmuir (a) and Freundlich (b) isotherm models of lead and fluoride

The best fitting non-linearised isotherm models for lead and fluoride adsorption are seen in Figure 7 (a) & (b), respectively. It can be seen in Figure 7 (a) that the Langmuir isotherm model best fits lead adsorption onto bone char shown by the data points. The Freundlich isotherm model best fits fluoride adsorption onto bone char, seen in Figure 7 (b).

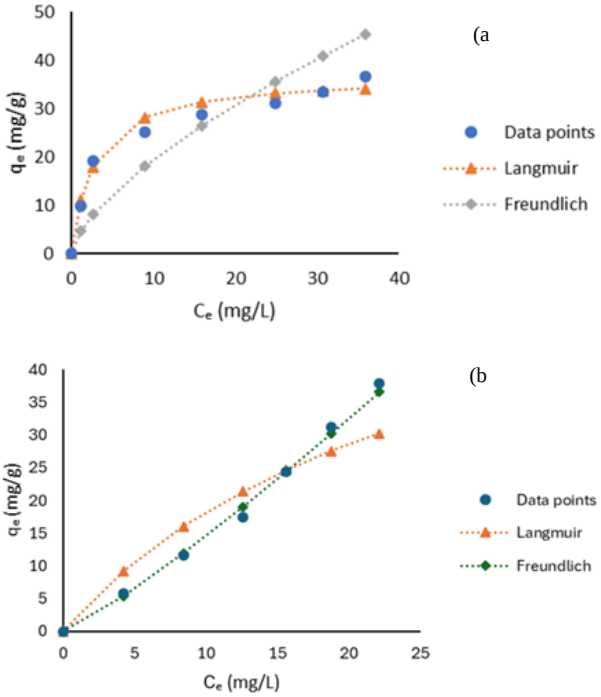

Fig. 7 Isotherm models of lead (a) and fluoride (b)

D.Kinetics Modelling

The adsorption kinetics of lead and fluoride were tested on the first- and second-order kinetics to determine the rate of adsorbent uptake onto bone char. Figure 8 (a) is the graph of the first-order kinetics model and Figure 8 (b) is the graph of the second-order kinetics model which is the best fitting model in agreement with [20,21] for lead and fluoride adsorption respectively, seen by the high R^2 values, 0.957 for lead and 0.967 for fluoride, compared to those of the first-order kinetics model. The adsorption kinetics parameters are listed in Table III. The kinetics rate constants (k_2) of the second-order kinetics model assumes the rate of adsorption to be proportional to the number and the square of the number of the free sites. The k_2 values for lead and fluoride adsorption are 0.001 and 0.002 g/mg.min, respectively.

TABLE II
ISOTHERM MODELS PARAMETERS OF LEAD AND FLUORIDE

Inorganic ions	Langmuir model			Freundlich model		
	q_m(mg/g)	b(L/mg)	R^2	1/n	k(mg/g)	R^2
Pb	36.765	0.365	0.984	0.660	4.259	0.646
F	66.667	0.038	0.208	1.160	1.008	0.999

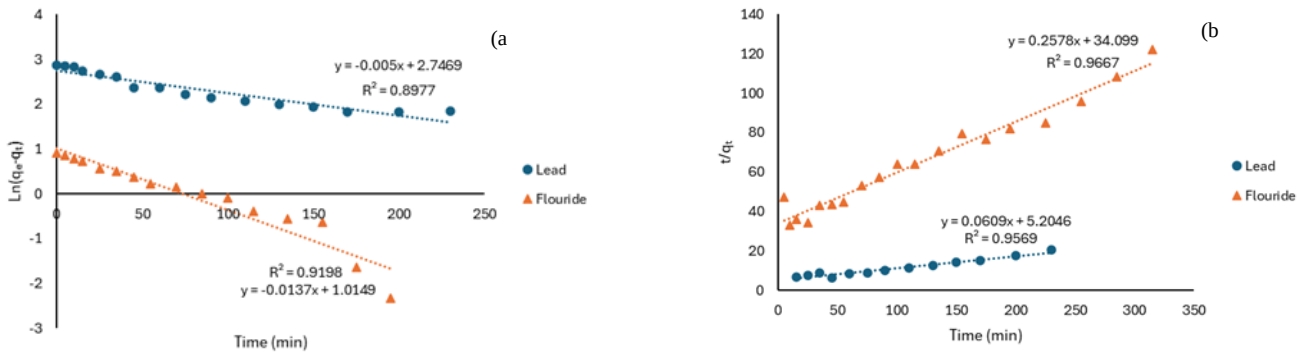

Fig. 8 Linear first order (a) and second order (b) kinetics models of lead and fluoride

TABLE III
KINETICS MODEL PARAMETERS OF LEAD AND FLUORIDE

	First-order kinetics			Experimental value	Second-order kinetics		
Inorganic ions	k_1 (min^{-1})	q_e^{cal}(mg/g)	R^2	q_e^{exp}(mg/g)	k_2 (g/mg.min)	q_e^{cal}(mg/g)	R^2
Pb	0.005	15.594	0.898	11.228	0.001	16.420	0.957
F	0.014	2.759	0.920	2.581	0.002	3.879	0.967

E. Adsorption by Fixed-Bed Filtration

The relative (C_t/C_0) concentration of lead and fluoride in solution over time can be seen in Figure 9, where C_t = inorganic component concentration at time t and C_0 = inorganic component at time 0. This correlates to the efficiency of bone char adsorption in terms of the removal percentage. This indicates that the C_t/C_0 of lead in solution at the end of the experiment was 0.65 meaning 35% removal efficiency of bone char. Similarly for fluoride, a C_t/C_0 of 0.86 translates to a 16% removal efficiency.

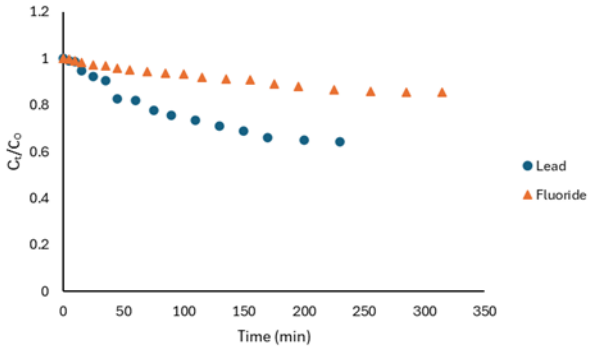

Fig. 9 Relative concentration of lead and fluoride in solution over time

The results of simulation of a water treatment system by removing lead and fluoride from water through adsorption onto fixed-bed bone char filtration system can be seen in Figure 10 through a breakthrough curve. The adsorption of lead was very rapid reaching 0.845 saturation in 10 minutes of running the experiment shown by the ratio of the concentration of lead at time t vs the concentration of lead at time 0 (C_t/C_0). This rapid adsorption is likely due to the attraction between the positively charged lead ions and the negatively charged bone char due to the solution pH = 6.72

which is above the 6.18 bone char pH PZC. After that adsorption continued over time until bone char reached a lead equilibrium saturation of 0.892 when the experiment ended. On the contrary, fluoride adsorption was not rapid, and this can be seen by the gradual increase in saturation of fluoride on bone char. At the time of ending the experiment the relative concentration of adsorbed fluoride was 0.486 and this indicates that fluoride had not yet saturated the bone char and that more fluoride could have been adsorbed with increase in time of the experiment.

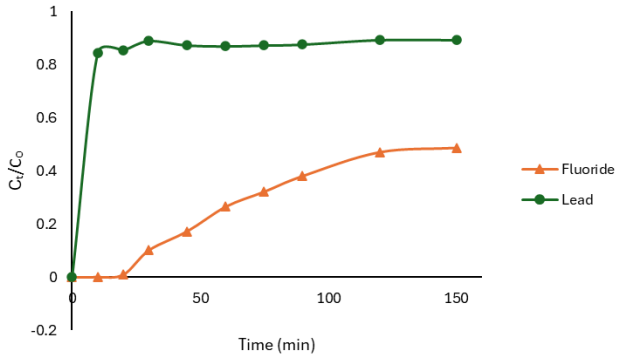

Fig. 10 Relative concentration of lead and fluoride adsorbed onto bone char over time

IV. CONCLUSION

The synthesis of bone char containing a high content of hydroxyapatite was successful, and this was proven by characterization results that revealed the presence of elemental components that make-up the mineral compound which is found in bone and subsequently bone char. Bone char was able to treat water synthetically contaminated with lead and fluoride ions by adsorption of the ions onto bone char. Lead adsorption fit the Langmuir isotherm model which assumes monolayer

adsorption on homogenously distributed site, whereas fluoride adsorption fit the Freundlich isotherm model which assumes reversible multi-layer adsorption on a heterogenous surface. Lead and fluoride adsorption both fit the second-order kinetics model which assumes the rate of adsorption to be proportional to the number and the square of the number of the free sites. Water treatment using the process of adsorption by filtering a lead and fluoride solution through a fixed bed of bone char was successful; in that the bone char was able to rapidly adsorb lead ions until saturation was reached; and gradually adsorb fluoride ions without reaching saturation at the time the experiment ended. Adsorption of fluoride through the fixed-bed bone char filter system would have to be done over a longer time to see when saturation will be reached.

REFERENCES

[1] Mpenyana-Monyatsi L, Mthombeni NH, Onyango MS, Momba MNB. Cost-effective filter materials coated with silver nanoparticles for the removal of pathogenic bacteria in groundwater. Int J Environ Res Public Health 2012;9:244–71. https://doi.org/10.3390/ijerph9010244.

[2] Singh R, Chadetrik R, Kumar R, Bishnoi K, Bhatia D, Kumar A, et al. Biosorption optimization of lead(II), cadmium(II) and copper(II) using response surface methodology and applicability in isotherms and thermodynamics modeling. J Hazard Mater 2010;174:623–34. https://doi.org/10.1016/j.jhazmat.2009.09.097.

[3] Zhao X, Yu Y, He M, Qu B, Shi H. Immobilization of Pb and Cd in Contaminated Soil Using Nano-Crystallite Hydroxyapatite. Procedia Environ Sci 2013;18:657–65. https://doi.org/10.1016/j.proenv.2013.04.090.

[4] Bhatnagar A, Kumar E, Sillanpää M. Fluoride removal from water by adsorption—A review. Chemical Engineering Journal 2011;171:811–40. https://doi.org/10.1016/j.cej.2011.05.028.

[5] Alkurdi SSA, Al-Juboori RA, Bundschuh J, Hamawand I. Bone char as a green sorbent for removing health threatening fluoride from drinking water. Environ Int 2019;127:704–19. https://doi.org/10.1016/j.envint.2019.03.065.

[6] Hadi P, To MH, Hui CW, Lin CSK, McKay G. Aqueous mercury adsorption by activated carbons. Water Res 2015;73:37–55. https://doi.org/10.1016/j.watres.2015.01.018.

[7] Hagemann N, Spokas K, Schmidt HP, Kägi R, Böhler MA, Bucheli TD. Activated carbon, biochar and charcoal: Linkages and synergies across pyrogenic carbon's ABCs. Water (Basel) 2018;10. https://doi.org/10.3390/w10020182.

[8] Purevsuren B, Davaajav Y, Namkhainorov J, Genadiev V. Pyrolysis of animal bone, characterization of the obtained char and tar and application of bone tar for crosslinking of epoxy resin. Bulgarian Chemical Communications 2017;49:34–9.

[9] Mousa SM, Ammar NS, Ibrahim HA. Removal of lead ions using hydroxyapatite nano-material prepared from phosphogypsum waste. Journal of Saudi Chemical Society 2016;20:357–65. https://doi.org/10.1016/j.jscs.2014.12.006.

[10] Deydier E, Guilet R, Sharrock P. Beneficial use of meat and bone meal combustion residue: "An efficient low cost material to remove lead from aqueous effluent." J Hazard Mater 2003;101:55–64. https://doi.org/10.1016/S0304-3894(03)00137-7.

[11] Rojas-Mayorga CK, Bonilla-Petriciolet A, Aguayo-Villarreal IA, Hernández-Montoya V, Moreno-Virgen MR, Tovar-Gómez R, et al. Optimization of pyrolysis conditions and adsorption properties of bone char for fluoride removal from water. J Anal Appl Pyrolysis 2013;104:10–8. https://doi.org/10.1016/j.jaap.2013.09.018.

[12] Ellingham STD, Thompson TJU, Islam M. Thermogravimetric analysis of property changes and weight loss in incinerated bone. Palaeogeogr Palaeoclimatol Palaeoecol 2015;438:239–44. https://doi.org/10.1016/j.palaeo.2015.08.009.

[13] Lambert JB, Shurvell HF, Lightner DA, Cooks RG. Introduction to Organic Spectroscopy. New York: Macmillan; 1987.

[14] Bedin KC, de Azevedo SP, Leandro PKT, Cazetta AL, Almeida VC. Bone char prepared by CO2 atmosphere: Preparation optimization and adsorption studies of Remazol Brilliant Blue R. J Clean Prod 2017;161:288–98. https://doi.org/10.1016/j.jclepro.2017.05.093.

[15] Nigri EM, Bhatnagar A, Rocha SDF. Thermal regeneration process of bone char used in the fluoride removal from aqueous solution. J Clean Prod 2017;142:3558–70. https://doi.org/10.1016/j.jclepro.2016.10.112.

[16] Shahid MK, Kim JY, Choi YG. Synthesis of bone char from cattle bones and its application for fluoride removal from the contaminated water. Groundw Sustain Dev 2019;8:324–31. https://doi.org/10.1016/j.gsd.2018.12.003.

[17] Lurtwitayapont S, Srisatit T. Comparison of Lead Removal by Various Types of Swine Bone Adsorbents. EnvironmentAsia 2010;3:32–8. https://doi.org/10.14456/ea.2010.32.

[18] Hu J, Wu D, Rao R, Liu R, Lai W. Adsorption kinetics of fluoride on bone char and its regeneration. Environment Protection Engineering 2020;43:93–112. https://doi.org/10.37190/epe170306.

[19] Medellin-Castillo NA, Leyva-Ramos R, Padilla-Ortega E, Perez RO, Flores-Cano J V., Berber-Mendoza MS. Adsorption capacity of bone char for removing fluoride from water solution. Role of hydroxyapatite content, adsorption mechanism and competing anions. Journal of Industrial and Engineering Chemistry 2014;20:4014–21. https://doi.org/10.1016/j.jiec.2013.12.105.

[20] Li G, Zhang J, Liu J. Adsorption characteristics of Pb (II) onto red clay, bentonite and bone char. IOP Conf Ser Earth Environ Sci 2020;526. https://doi.org/10.1088/1755-1315/526/1/012018.

[21] El Hamri R, Taitai A, Mourabet M, El Boujaady H, Bennani-Ziatni M, El Rhilassi A. Removal of fluoride from aqueous solution by adsorption on hydroxyapatite (HAp) using response surface methodology. Journal of Saudi Chemical Society 2012;19:603–15. https://doi.org/10.1016/j.jscs.2012.03.003.